

Data-driven adaptive building thermal controller tuning with constraints: A primal-dual contextual Bayesian optimization approach

Wenjie Xu^{a,b}, Bratislav Svetozarevic^a, Loris Di Natale^{a,b}, Philipp Heer^a and Colin N Jones^b

^aUrban Energy Systems Laboratory, Swiss Federal Laboratories for Materials Science and Technology (Empa), 8600 Dübendorf, Switzerland

^bLaboratoire d'Automatique, Swiss Federal Institute of Technology Lausanne (EPFL), 1015 Lausanne, Switzerland

ARTICLE INFO

Keywords:

Building Thermal Control
Controller Tuning
Bayesian Optimization
Contextual Model
Primal-Dual Method

Abstract

We study the problem of tuning the parameters of a room temperature controller to minimize its energy consumption, subject to the constraint that the daily cumulative thermal discomfort of the occupants is below a given threshold. We formulate it as an online constrained black-box optimization problem where, on each day, we observe some relevant environmental context and adaptively select the controller parameters. In this paper, we propose to use a data-driven **Primal-Dual Contextual Bayesian Optimization (PDCBO)** approach to solve this problem.

In a simulation case study on a single room, we apply our algorithm to tune the parameters of a Proportional Integral (PI) heating controller and the pre-heating time. Our results show that PDCBO can save up to 4.7% energy consumption compared to other state-of-the-art Bayesian optimization-based methods while keeping the daily thermal discomfort below the given tolerable threshold on average. Additionally, PDCBO can automatically track time-varying tolerable thresholds while existing methods fail to do so. We then study an alternative constrained tuning problem where we aim to minimize the thermal discomfort with a given energy budget. With this formulation, PDCBO reduces the average discomfort by up to 63% compared to state-of-the-art safe optimization methods while keeping the average daily energy consumption below the required threshold.

1. Introduction

With the increasing challenge of climate change, the high energy usage in the building sector calls for the development of energy-efficient control solutions. On the other hand, it is also critical to meet the comfort requirement of the occupants [1]. While advanced control methods have been developed (e.g., model predictive control [2–4] and reinforcement learning [5–9]) to optimize the energy consumption and/or the comfort of the occupants, simple rule-based controllers (e.g., bang-bang or Proportional Integral Derivative PID controllers) still dominate the current practice [5]. The parameters of these controllers are typically set manually by building engineers and kept fixed for the life of the building. However, these hand-tuned simple rule-based controllers have two main limitations in practice.

The first limitation is *sub-optimality*. It is generally hard to explicitly model the effect of given control parameters on the performance (the energy consumption and thermal comfort of the occupants) to optimize them. Consequently, manually tuned controllers usually operate suboptimally [10, 11], potentially incurring excessively high discomfort or energy consumption.

The other limitation is *non-adaptivity*. Given the influence of external factors, typically the weather conditions, an optimal building control policy should intuitively be able to adapt to environmental changes. Previous works indeed indicated that adaptive controller parameters can bring significant energy savings (e.g., in [12]). However, the

parameters of rule-based controllers are typically set during commissioning and then kept fixed.

Meanwhile, with more and more ubiquitous sensing technology [13], we can monitor the operations of buildings online. By collecting the temperature and heating power trajectories, building control performance, including energy consumption and occupant comfort, can be evaluated on each day.

Based on the above observations, it is of great practical interest to be able to adaptively tune building controller parameters to optimize their online performance. Since we are interested in minimizing both the energy consumption and the thermal discomfort of the occupants, tuning these parameters is a multi-objective problem. Furthermore, the two objectives are often in contradiction, with improved thermal comfort typically coming at the cost of additional energy consumption, making the tuning procedure challenging in general.

In this work, we formulate it as an online constrained optimization problem, where one metric — the energy consumption or the thermal discomfort — is set as the objective and the other as the constraint. On each day, we solve an online problem to get a new set of controller parameters and apply them to the building. However, solving this constrained problem poses several new challenges.

Constraint violation management. It is generally difficult, if even possible, to strictly satisfy the comfort or energy constraints at all times since the effect of the control parameters on the energy consumption or the thermal comfort is hard to predict accurately. However, thanks to the soft nature of these constraints, some violations are acceptable in practice. Interestingly, short-term constraint violations can be beneficial to efficiently identify the optimal set of

*Corresponding author: wenjie.xu@epfl.ch (Wenjie Xu), Laboratoire d'Automatique, Swiss Federal Institute of Technology Lausanne (EPFL), 1015 Lausanne, Switzerland

ORCID(s): 0000-0001-7475-0056 (W. Xu)

parameters, as shown in previous works [14, 15]. Despite the benefits of short-term constraint violation, we still want to ensure constraint satisfaction in the long term.

Cumulative constraint satisfaction. While the thermal comfort of the occupants has to be monitored every day, an energy consumption constraint only makes sense when it is accumulated over certain periods. That is to say, despite tuning the parameters of the controller every day, we want the cumulative energy consumption to be small during a season or a year, for example, rather than on each day. Indeed, it is expected that the system has to consume more energy on cold days than on warm ones to optimize the comfort of the occupants.

Time-varying constraint tracking. Due to changes in energy prices or occupant behaviors, the preference for energy saving or comfort may change. Existing learning-based methods (e.g., [5]) may need to train a controller from scratch again, which can be very time-consuming and data-intensive. It is desired that the tuning algorithm can respond to such changes of preference rapidly.

Bayesian optimization (BO), as a sample-efficient method to optimize black-box functions [16, 17] by constructing a stochastic surrogate model, is a promising method to solve the building controller tuning problem. However, the vanilla Bayesian optimization method is not readily applicable to address all the aforementioned challenges. In addition, black-box constraints and environmental disturbances need to be incorporated.

In this paper, we propose to use our recently proposed primal-dual contextual Bayesian optimization (PDCBO) [18] method to automatically and adaptively tune the parameters of a Proportional Integral (PI) controller, the daytime setpoint temperature, and the pre-heating time for building thermal control with time-varying ambient conditions. PDCBO has been shown to asymptotically achieve the *optimal* performance while *satisfying constraints* on average by adapting to the time-varying environmental changes, which are modeled as contexts in [18]. Specifically, our contributions are:

1. The adaptive building controller tuning problem is modeled as an online constrained black-box optimization problem and is then solved with PDCBO method.
2. Simulation results show that PDCBO can simultaneously optimize the energy consumption and keep the discomfort level below a user-defined upper bound on average in the long term, contrary to other state-of-the-art constrained BO methods.
3. When the discomfort threshold is time-varying, PDCBO is again the only method able to rapidly adapt to the threshold changes and track the constraints well. This highlights the capability of PDCBO to automatically explore the allowable discomfort level in order to reduce energy consumption.
4. When we instead aim to minimize the discomfort subject to the daily average energy consumption being within a given budget, simulation results show that

PDCBO [18] reduces the average discomfort by about 63% compared to other safe BO method.

2. Related Work

Existing research in the multi-objective building optimization literature typically uses a weighted sum of discomfort and energy consumption as the performance target when designing or learning building controllers, e.g. in [2, 5, 19–21]. However, with such a formulation, there is no systematic way of choosing the weighting factor between the two objectives. Random weights may lead to undesirable consequences, such as intolerable discomfort for the occupants or excessive energy usage with very marginal comfort improvement.

Some research used Pareto optimization [22–24], where a set of trade-off optimal solutions — on the Pareto front — are derived. However, this approach is typically sample inefficient, since a good approximation of a Pareto front takes a significant number of Pareto optimal points. Furthermore, Pareto optimization typically does not consider the performance during the optimization process and as such cannot be deployed to tune the parameters of real-world building systems online, where the online performance during tuning also needs to be guaranteed. We refer the reader to [25] for a detailed review of simulation-based optimization methods applied to building performance analysis.

Compared to existing weighted-sum formulations, our online constrained optimization formulation is more desirable due to the following reasons:

More predictable solutions. Different from the weighted sum formulation, which may lead to undesirable and unpredictable outcomes with a random weight, the optimal solution of a constrained problem always respects the constraints (e.g., daily discomfort upper bounded by a threshold) while minimizing the objective (e.g., energy consumption).

Easy for preference personalization. Different occupants may have different preferences towards comfort and energy saving. Some occupants may want strictly comfortable temperatures regardless of energy consumption. Others may be less sensitive to the temperature and willing to trade some comfort for more energy savings. In a weighted-sum formulation, how to set the weights according to such energy-discomfort preferences is unclear quantitatively, whereas, in a constrained formulation, it can be easily captured by modifying the constraint on discomfort or energy.

Energy consumption modeling is a critical problem for building control [26]. For BO, we use Gaussian process to learn the black-box mapping from control parameters to the closed-loop energy consumption and discomfort due to its high sample efficiency and minimal human effort. BO has already been applied to many different energy systems (including building) optimization problems, such as model calibration [27, 28], chiller plant controller [29], process control [30], battery charging [31], and turbine design [32].

However, existing applications of Bayesian optimization-based methods either have no constraint consideration at all or can not guarantee long-term constraint feasibility.

One of the most popular methods, Constrained Expected Improvement (CEI) [33, 34], encodes the constraint information in the acquisition function. This method is however not able to guarantee the satisfaction of the desired constraints. To deal with hard safety-critical constraints, Safe BO restricts the sampling inside a safe set where feasibility is guaranteed with high probability [35]. More recently, [36] proposed a primal-dual algorithm to solve the constrained Bayesian optimization problem, which has theoretical bounds on the cumulative regret and soft violation. As an extension to handle contextual inputs, **Primal Dual Contextual Bayesian Optimization** (PDCBO) was recently developed [18]. In this paper, we propose using PDCBO to solve the controller parameter optimization problem.

3. Problem Statement

We consider an online constrained building controller tuning problem where the parameters are modified each day.

Controller structure We consider a PI controller to govern the heating of a room, which is currently a common practice in building automation systems. The control law is given as,

$$u(t) = K_p e(t) + K_i \int_0^t e(\tau) d\tau,$$

where K_p is the proportional gain, K_i is the integral gain, $e(t) := T_{\text{setpoint}}(t) - T(t)$ is the difference between the temperature setpoint and the measured temperature T at time t , and $u(t)$ (after truncated to the interval $[0, 1]$) is the control input. In our case, the latter represents the heating power of the room. To incorporate the different thermal requirements during daytime and nighttime — e.g., to leverage the fact that the building is vacant at night —, we adopt a lower setpoint during the night than at daytime.

Tuning variables Our tuning variables include the proportional and integral gains of the PI controller, and the daytime setpoint temperature. To incorporate pre-heating behaviors, we also include the switching time from nighttime mode to daytime mode as a tuning variable. On the other hand, we fix the nighttime setpoint to 22.5°C, which is inside the comfort range of 20°C to 23.5°C in ASHRAE 55-1992 [37] and thus a reasonable choice, and the switching time from daytime mode to nighttime mode at 6 PM, which is a typical end-of-work time. We use θ to denote the tuning parameter, which is the concatenation of all tuning variables.

Contextual variables We consider the most critical environmental factors, namely the forecasted average daily ambient temperature and ambient solar irradiation, as contextual inputs of PDCBO. We also include the initial temperature at the start of each day (midnight) as an additional contextual

variable. We use z_n to denote the concatenated contextual variables on the day n .

Since the true average ambient temperature and solar irradiation can not be obtained before selecting the new control parameters in reality, we can use the forecast average ambient temperature T_n^{ambient} and forecast average solar irradiation I_n , on each day n . The initial room temperature T_n^{init} is also measured. The contextual variables are given as $z_n = (T_n^{\text{ambient}}, I_n, T_n^{\text{init}})$.

Discomfort quantification Similar to what is done in many existing learning-based building control works (e.g., [5]), we define and quantify the discomfort of the occupants as the cumulative temperature deviations from the potentially time-varying comfortable temperature range $[T_{\min}(t), T_{\max}(t)]$:

$$c_{\text{discomfort}}(T, t) = \begin{cases} 0, & \text{if } T_{\min}(t) \leq T \leq T_{\max}(t), \\ T - T_{\max}(t), & \text{if } T > T_{\max}(t), \\ T_{\min}(t) - T, & \text{if } T < T_{\min}(t), \end{cases}$$

We use D_n to denote the cumulative discomfort on day n , namely the integration of $c_{\text{discomfort}}$ over day n :

$$D_n = \int_{\text{day } n} c_{\text{discomfort}}(T(t), t) dt. \quad (1)$$

Similarly, we compute the energy consumption over a day as:

$$E_n = \int_{\text{day } n} p(t) dt, \quad (2)$$

where $p(t)$ is the power at time t , which is proportional to $u(t)$. Since both E_n and D_n are unknown functions of θ and z_n corrupted by noise, we introduce Gaussian processes to model them as follows:

$$E_n = J(\theta_n, z_n) + v_n^J, \quad (3a)$$

$$D_n = g(\theta_n, z_n) + v_n^g, \quad (3b)$$

where J is assumed to be sampled from the Gaussian process $\mathcal{GP}(\mu_J, k_J(\cdot, \cdot))$ with prior mean μ_J and prior covariance $k_J(\cdot, \cdot)$ and g is constructed similarly. Furthermore, $v_n^J \sim \mathcal{N}(0, \sigma_J^2)$ and $v_n^g \sim \mathcal{N}(0, \sigma_g^2)$ are independent identically distributed Gaussian noises.

Constrained optimization problem. On the day n , we aim to adaptively select a set of parameters θ_n by solving the following online constrained optimization problem,

$$\min_{\theta \in \Theta} J(\theta, z_n), \quad (4a)$$

$$\text{subject to: } g(\theta, z_n) \leq D^{\text{thr}}, \quad (4b)$$

where Θ is the set of candidate control parameters (e.g., a hyperbox) and D^{thr} is the maximum amount of allowed

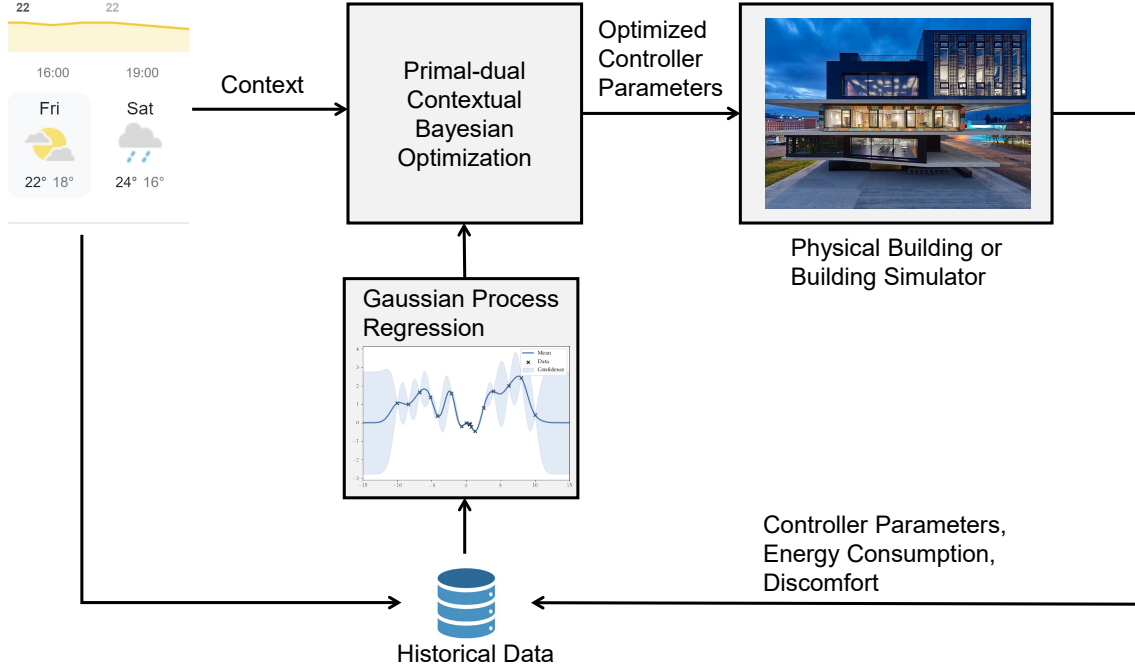


Figure 1: Overview of the proposed controller tuning method. On each day, we get the average temperature and average solar irradiation prediction from given weather forecasts. With the forecasted contexts and the Gaussian process surrogate model, PDCBO selects a new set of optimized controller parameters to run the black-box building simulator or conduct a physical experiment. We then collect the new discomfort and energy consumption data and update their GP posteriors. At the same time, we update the dual variables with the constraints information.

comfort violations. Both the objective and the constraint are unknown black-box functions of the control parameter θ and the contextual variable z , which need to be learned online during a period. Alternatively, we get the energy-constrained discomfort minimization formulation by setting g to be the objective and J to be below a threshold in the constraint as shown in Eq. 5.

$$\min_{\theta \in \Theta} g(\theta, z_n), \quad (5a)$$

$$\text{subject to: } J(\theta, z_n) \leq E^{\text{thr}}, \quad (5b)$$

where E^{thr} is the energy budget.

Performance metric. Although the problem (4) is formulated as an online problem with instantaneous objective and constraints, we measure the performance of the algorithm using the whole closed-loop trajectory $\{(\theta_n, z_n)\}_{n=1}^N$. Overall, the metric is the cumulative objective function during a period N , that is $\sum_{n=1}^N J(\theta_n, z_n)$, while respecting the constraints $g(\theta_n, z_n) \leq D^{\text{thr}}$ on average. To compare the performance of each algorithm, we introduce two running average metrics,

$$E_n^{\text{avg}} := \frac{1}{n} \sum_{k=1}^n E_k, \quad (6a)$$

$$D_n^{\text{avg}} := \frac{1}{n} \sum_{k=1}^n D_k. \quad (6b)$$

4. Methodology

Fig. 1 demonstrates an overview of the proposed methodology. On each day n , we collect the contextual information z_n and use the algorithm detailed in the following sections to choose θ_n . We then run the simulation for the next day with this set of parameters and calculate E_n and D_n using the power input and temperature trajectories obtained from simulation or real-world operation. We then update the Gaussian Processes (GPs) with the new data, obtain the context of the next day, and sample new control parameters.

Note that, given the online setting, this methodology could also directly be applied to a real building, bypassing the need for simulation studies. In this section, we will focus on the Prob. (4). The same algorithm can be similarly applied to Prob. (5).

4.1. Preliminaries

Gaussian process regression We learn J and g using GP regression, which is a sample-efficient method to approximate nonlinear functions. Denoting the set of historical data

$$\mathcal{H}_n := \{(E_\tau, D_\tau, T_\tau^{\text{ambient}}, I_\tau, T_\tau^{\text{init}}, \theta_\tau)_{\tau=1}^{n-1}\}$$

and $x := (\theta, z)$, we can derive the posterior distribution of J on day n as a Gaussian random variable with mean and variance given as [38]

$$\mu_J(x|\mathcal{H}_n) = k_J^\top(x, x_{1:n-1})(K_J + \sigma_J^2 I)^{-1} \Delta y_J + \mu_J(x), \quad (7a)$$

$$\sigma_J^2(x|\mathcal{H}_n) = k_J(x, x) \quad (7b)$$

$$-k_J^\top(x, x_{1:n-1})(K_J + \sigma_J^2 I)^{-1} k_J(x_{1:n-1}, x),$$

where $\Delta y_J = E_{1:n-1} - \mu_J(x_{1:n-1})$. The posterior Gaussian distribution of g can be similarly derived. We refer the readers to [39] for more details on Gaussian process regression.

Bayesian optimization (BO) Bayesian optimization is a derivative-free black-box optimization method (see [40]) which iteratively

1. Samples a point to evaluate the black-box function;
2. Uses *all* the historical samples to construct a surrogate model of the black-box function with GPs.
3. Finds a new sample that is promising to improve the objective by solving an auxiliary problem constructed with the surrogate model.

For unconstrained Bayesian optimization, a popular way to construct this auxiliary problem in step 3 is minimizing the *lower confidence bound* [41]¹ of the objective, which is defined as

$$\mu_J(x|\mathcal{H}_n) - \beta_n^{1/2} \sigma_J(x|\mathcal{H}_n), \quad (8)$$

where $\beta_n^{1/2}$ is a positive weighting coefficient that balances exploitation and exploration. The larger β_n is, the more likely points with large posterior variance — i.e., uncertainty — will be sampled.

4.2. PDCBO

PDCBO is based on the lower confidence bounds constructed from the posterior distribution of the energy consumption and thermal discomfort:

$$\underline{J}_n(\theta, z_n) = \mu_J(\theta, z_n|\mathcal{H}_n) - \beta_n^{1/2} \sigma_J(\theta, z_n|\mathcal{H}_n), \quad (9a)$$

$$\underline{g}_n(\theta, z_n) = \mu_g(\theta, z_n|\mathcal{H}_n) - \beta_n^{1/2} \sigma_g(\theta, z_n|\mathcal{H}_n), \quad (9b)$$

where z_n is the observed context at step n and $\beta_n^{1/2}$ is the positive coefficient which balances the tradeoff between exploitation and exploration, where exploitation is captured by the posterior mean and the exploration is captured by the posterior standard deviation.

Note that while [18] proposed a rigorous way to select β_n — which increases at each time step — it can typically be set to be a constant in practice.

We then relax the constraint in the problem (4) and write out the corresponding Lagrangian:

$$\mathcal{L}(\theta, z_n, \lambda) = J(\theta, z_n) + \lambda g(\theta, z_n), \quad (10)$$

where λ is the corresponding dual variable. Following classical ideas from the constrained optimization literature [42], we consider the corresponding max-min problem,

$$\max_{\lambda} \min_{\theta} \mathcal{L}(\theta, z_n, \lambda). \quad (11)$$

Since both J and g are black-box functions, we use (9) to approximate them and solve the inner minimization problem. For the outer maximization problem, on the other hand, we

Algorithm 1 PDCBO for building controller tuning

- 1: **Require:** Running horizon N , initial dual variable λ_1
 - 2: **for** $n \in [N]$ **do**
 - 3: Observe the context $z_n = (T_n^{\text{ambient}}, I_n, T_n^{\text{init}})$
 - 4: **Primal update:**
 $\theta_n \in \arg \min \{ \underline{J}_n(\theta, z_n) + \lambda_n \underline{g}_n(\theta, z_n) \}$
 - 5: **Dual update:**
 $\lambda_{n+1} = [\lambda_n + \eta(g_n(\theta_n, z_n) - D^{\text{thr}}) + \epsilon]^+$
 - 6: Update the control parameters to θ_n , run the closed-loop simulation/experiment, and append the new data $(E_n, D_n, T_n^{\text{ambient}}, I_n, T_n^{\text{init}}, \theta_n)$ to \mathcal{H}_n .
 - 7: Update the GP posteriors of J and g .
 - 8: **end for**
-

apply a standard dual ascent step, as detailed in Algorithm 1, where η is the step size and ϵ is a small constant shift.

In sharp contrast to existing weighted-sum formulations in model predictive control [2] or reinforcement learning [5] based building control methods, where the weight is static, the weight λ_n in Alg. 1 is adaptively adjusted each day according to the measurements of the constrained metric. Intuitively, if the constraint threshold is violated during one day, the weighting factor will be increased to penalize the constraint more in the next step. Such adaptivity of the weight leads to the automatic balance of energy consumption and discomfort. In the dual update, we also add a constant drift ϵ to prevent the dual variable from being too small, which would mean the optimization problem does not consider any constraint anymore and might incur severe violations.

In this paper, we solve the auxiliary problem in the primal-update step in line 4 with a grid search algorithm over the set Θ . This is feasible since we are dealing with low dimensions — $\theta \in \mathbb{R}^4$ —, and evaluating both lower confidence bound functions is computationally inexpensive.

4.3. Theoretical Guarantees

We now restate theoretical guarantees for the performance of Alg. 1, as shown in [18].

Theorem 1 (Theorem 6.1, [18]). *For kernels with sublinear maximum information gain term (see [41]) and sufficiently large N , by properly setting η and ϵ as shown in [18], we have,*

$$\sum_{n=1}^N (J(\theta_n, z_n) - J(\theta^*(z_n), z_n)) = \mathcal{O} \left((\gamma_N^J + \gamma_N^g) \sqrt{N} \right), \quad (12)$$

where $\theta^*(z_n)$ is the optimal solution of the Prob. (4) with contextual variable z_n , γ_N^J , γ_N^g (γ_N^g , resp.) is the maximum information gain, which measures the complexity of the unknown

¹Note that the work [41] uses the upper confidence bound instead of the lower one since they consider the problem of maximizing J instead of minimizing it.

black-box function J (g , resp.) [41]. And,

$$\frac{\sum_{n=1}^N g(\theta_n, z_n)}{N} \leq D^{\text{thr}}. \quad (13)$$

Theorem 1 guarantees that the cumulative gap between the parameters selected by our algorithm and the ground truth time-varying optimal parameters is upper bounded by $\mathcal{O}((\gamma_N^J + \gamma_N^g)\sqrt{N})$. Furthermore, the threshold constraint on g is satisfied on average as shown in (13). We refer the interested reader to the theoretical paper [18] for more details. Specifically, for the commonly used squared exponential (SE) prior covariance functions, the cumulative suboptimality bound reduces to $\mathcal{O}((\log N)^{d+1}\sqrt{N})$ [41], which is sublinear. Therefore, the average suboptimality converges to zero, i.e., PDCBO achieves asymptotic optimality on average.

Specific to the building application considered in this paper, Theorem 1 highlights that PDCBO can asymptotically achieve the *optimal* building control performance while *satisfying constraints* on average.

5. Implementations and Results

In this section, we present some implementation details and then provide simulation results, comparing the performance of PDCBO, state-of-the-art constrained BO methods, and fixed control parameters. We consider both the discomfort-constrained energy minimization problem and the energy-constrained discomfort minimization problem.



Figure 2: NEST building, Duebendorf, with the UMAR unit in white circle. © Zoey Braun, Stuttgart.

5.1. Implementation details

Building simulator In this work, we consider the control of the temperature of a single room located in the ‘Urban Mining and Recycling’ (UMAR) unit, pictured in Fig. 2. It is equipped with radiant heating/cooling panels, where hot/cold water is circulated when a valve is opened. We use a digital twin of the room, based on a Physically Consistent Neural Network (PCNN) [43], as our simulator for evaluation. Despite relying on Neural Networks (NNs), PCNNs

Table 1

The choice of hyperparameters for squared exponential kernel, where the heating start time is in the unit of minute.

	σ_{SE}^2	Lengthscale in P (log-scale)	Lengthscale in I (log-scale)	Lengthscale in daytime setpoint	Lengthscale in heating start time
J	56.7	5.9	3.1	2.7	1290.6
g	546.1	6.0	8.8	5.2	1188.0

respect the underlying physical laws *by design* while simultaneously achieving state-of-the-art modeling accuracy. In our case, the physical consistency ensures that heating a room increases its temperature, as expected, in contrast to what might happen with classical NNs [44]. This ensures our algorithm does not pick up spurious behaviors due to modeling inconsistencies. On the other hand, PCNNs attain superior prediction accuracy compared to classical physically consistent models [43, 44].

State-of-the-art baselines We compare our algorithm with two other state-of-the-art Bayesian optimization algorithms: SafeOPT [12] and CEI [33]. Both baseline algorithms also use Gaussian process to learn the mapping from the control parameters to the daily energy/discomfort. SafeOPT aims to not violate the constraints during the whole sampling process and thus is very cautious. CEI algorithm encodes the constraint implicitly in the auxiliary problem but does not explicitly consider feasibility. Therefore, CEI algorithm can be very aggressive and may violate the constraints severely. For fair comparison purposes, we extend both algorithms to the contextual setting. Specifically, similarly to the procedure described in Sec. 3 and Sec. 4.2, we augment the input space of the Gaussian processes with contextual variables for both SafeOPT and CEI.

Choice of parameters All the GPs use a squared exponential kernel, a common choice in BO applications (e.g., [14]):

$$k(\mathbf{x}, \mathbf{y}) = \sigma_{\text{SE}}^2 \exp \left\{ - \sum_{i=1}^d \left(\frac{x_i - y_i}{l_i} \right)^2 \right\}, \quad (14)$$

where σ_{SE}^2 captures the variation of the function to be modelled, l_i is the lengthscale that captures the variation rate in the i -th input variable, and d is the dimension of the input variable. We selected those hyperparameters as shown in Table 1 by doing maximum likelihood estimation (MLE) over an initial set of building operational data [39]. Concerning the parameters specific to PDCBO, we manually tried different values and set the dual update step size $\eta = 1$ and the lower confidence bound weight $\beta_t^{1/2} = 3$, which works well in this application. In this case study, ϵ is manually set to be 0, which does not significantly impact the constraint violations for this particular application.

Generation of contexts The initial temperature of the room is an internal state of the simulator. Ambient temperature and solar irradiation are from the real-world weather dataset recorded at the NEST building of Empa in Zurich. In this paper, we use perfect forecast information, i.e., the true average daily ambient temperature and solar irradiation

of the next day, as contextual inputs. When deploying our method online to the real world, however, real-world temperature and solar irradiation forecasts could be used.

Comfort range and energy price We adopt a much tighter comfort range (21°C to 24°C during the nighttime and 23°C to 24°C during the daytime) than the recommended comfort ranges [37] (e.g., 20°C to 23.5°C in ASHRAE 55-1992). Therefore, we allow larger cumulative temperature deviation to capture different levels of comfort requirements. To incorporate time-varying electricity prices, we penalize the day-time energy consumption twice, which approximately matches the real-world electricity tariff data [45].

Simulation In our experiments, 300 days are simulated to compare the performance of each controller during the heating season. Since the building needs to be cooled rather than heated over the summer and due to data missing issue, the days in our simulation may not be consecutive — we artificially stitch non-consecutive days together, using the last simulated room temperature of the previous day as initial value for the next one.

Note that control parameters need to be continuously adapted due to the time-varying contexts. So we use these running average metrics during the tuning process, instead of choosing one fixed solution over the whole running horizon.

The algorithms are implemented in python and we used GPy [46] to implement GPs. The code and data can be accessed on https://gitlab.nccr-automation.ch/wenjie.cuhk/pdco_room_temperature_controller_tuning.

5.2. Discomfort constrained energy minimization

5.2.1. Adaptivity Gain Compared to Static Parameters

To demonstrate how adaptivity of control parameters benefits the energy saving and discomfort reduction, Fig. 3 shows samples of the daily energy consumption and thermal discomfort of the PDCBO algorithm with discomfort threshold 9 K h. To account for the fact that more energy is naturally needed to maintain the inside temperature in a reasonable range when the temperature outside is lower, we plot both metrics against the mean ambient temperature in a day. For comparison purposes, we also plotted samples corresponding to fixed controller parameters that are manually set by experience. For better visualization, we also plot the linear regression results for both sets of samples. It can be seen that PDCBO can reduce both the energy consumption and the discomfort compared to static parameters. Interestingly, in the low ambient temperature regime ($\leq 10^\circ\text{C}$), the discomfort reduction is more significant while in the high ambient temperature regime, the energy reduction is more significant. This matches our intuition that uncaredful heating (e.g., not enough heating power) is more likely to lead to severe discomfort on cold days and thus, there is more room for discomfort reduction on cold days. Meanwhile, on warm days, overheating can be an issue with static control parameters and thus there is more room for energy reduction.

To understand how the parameters are chosen by PDCBO, the coefficients K_p and K_i and the switching time

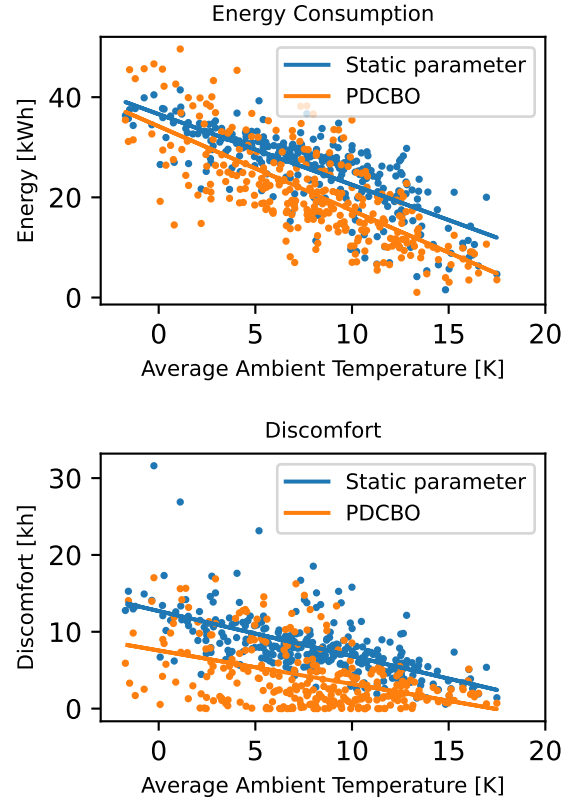


Figure 3: Comparison of energy consumption and discomfort with respect to the average ambient temperature.

from nighttime setpoint to daytime setpoint are also plotted against the average ambient temperature in Fig. 4. There is a trend to switch the setpoint earlier when the ambient temperature is low, which matches our intuition that pre-heating is needed to avoid low temperatures during working hours on cold days. Interestingly, in the low-temperature regime, PDCBO tends to favor parameters with small P and large I, contrary to the high-temperature regime. Intuitively, low ambient temperatures have a large ‘cooling’ effect on the room and, therefore, a large integral term is needed to accelerate the heating towards the set-point to reduce discomfort and also cancel out the severe offset caused by low ambient temperature. On the contrary, in the high ambient temperature regime, the ambient effect is less severe and small integral term can be adopted to avoid the overshoot and save energy. Meanwhile, a large proportional term can help reduce the offset issue in the high ambient temperature regime. Remarkably, such an adaptation policy is automatically found by our PDCBO algorithm.

5.2.2. Comparison with SafeOPT and CEI

Fig. 5 shows the daily average energy consumption and thermal discomfort obtained by the three methods over 300 days with three different discomfort thresholds $D^{thr} = 5, 10, \text{ or } 15$ K h per day, where 1 K h represents 1 Kelvin temperature deviation from comfortable range for 1 hour. As can be seen, PDCBO can keep the average discomfort below

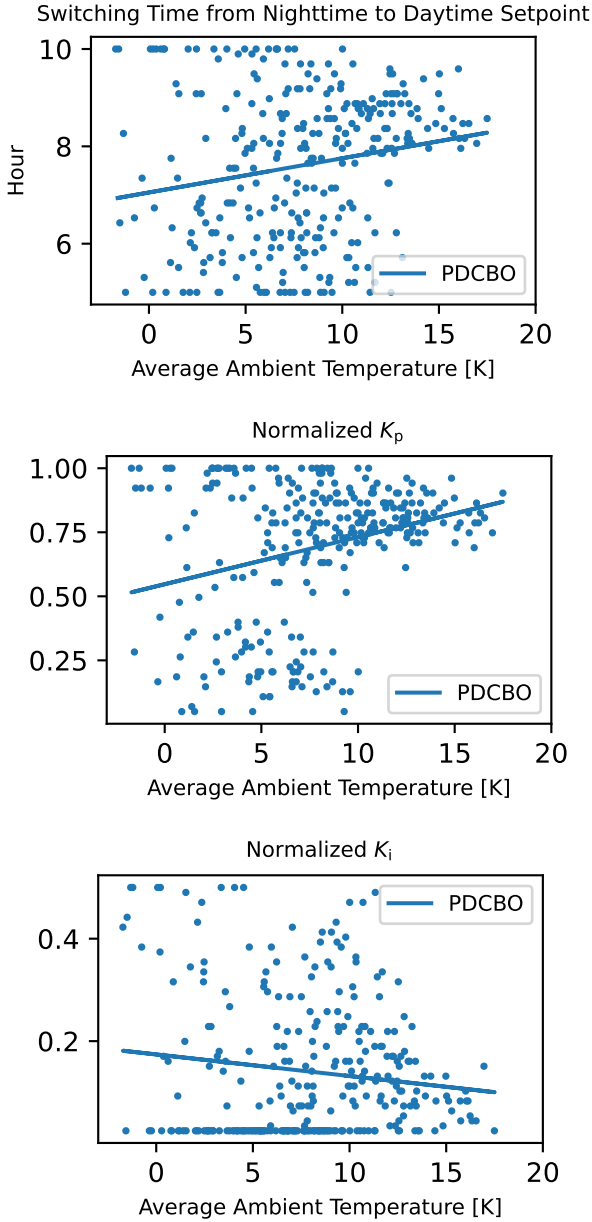


Figure 4: PDCBO samples of switching time, proportional gain K_p , and integral gain K_i with respect to ambient average temperature. Both the proportional gain and integral gain are normalized against a base value so that they are unitless.

the user-defined threshold in the long-term, contrary to CEI, which incurs severe comfort violations. On the other hand, PDCBO can achieve significant energy savings compared to SafeOPT. Indeed, our method uses the allowed maximum discomfort budget and exploits it to achieve more energy savings. In sharp contrast, SafeOPT is overly cautious and can not achieve all the potential energy savings given the allowed discomfort threshold.

Fig. 6 gives three-day sample trajectories of the temperature and the heating power after running for 70 days, with discomfort threshold at 5 K h. This confirms that SafeOPT is very cautious and does not explore the energy saving

Table 2

Discomfort violation percentage for CEI method over the whole running period of 300 days, which is defined as $\frac{\text{Average discomfort} - \text{Discomfort threshold}}{\text{Discomfort threshold}}$, where the average discomfort is defined as in Eq. (6b).

Discomfort threshold (K h)	5	10	15
Violation Percentage (%)	247	82	18

potential of lowering the temperature setpoints. On the other hand, CEI samples parameters aggressively, leading to large thermal discomfort. As a good compromise, PDCBO identifies control parameters that can simultaneously reduce the energy consumption and manage the discomfort well.

5.2.3. Impact of discomfort threshold

To visualize the impact of different thermal comfort thresholds, Fig. 7 presents the average daily energy consumption and comfort violations (i.e., the cumulative temperature violations from a comfort range) obtained by the three methods with a threshold changing from 5 K h to 25 K h. Note that the absolute value of the cumulative temperature deviation highly depends on the comfort range adopted. As given in Sec. 5.1, the comfort range we adopt is tighter than the standard range. Therefore, we can set the threshold of discomfort (quantified by cumulative temperature deviation) to be from a larger range to capture diversified comfort requirements. We also note that PDCBO consistently respects the discomfort threshold constraints in all cases in the long-term (except the minor violation when the discomfort threshold is 5 K h) while simultaneously leveraging the increasing allowed discomfort budget to reduce the energy consumption. Compared to SafeOPT, PDCBO saves up to 4.7% energy, as we increase the discomfort threshold to 25 K h. Meanwhile, when the discomfort threshold is small, CEI uses less energy than PDCBO but at the cost of severe comfort violations (Tab. 2), which can be strongly undesired by room occupants. However, when a large thermal discomfort is tolerable — when the constraint is easier to meet at 25 K h —, CEI can perform slightly better than PDCBO.

Remarkably, the average discomfort incurred by PDCBO significantly increases with larger discomfort thresholds D^{thr} while the average energy consumption decreases, demonstrating that our method can efficiently exploit the increased allowed thermal discomfort to save more energy. Such adaptivity to different requirements for comfort is critical since the occupants' preference for thermal comfort [47] and energy consumption can be diverse in practice. On the contrary, the other two baseline methods are either too cautious (SafeOPT) or overly aggressive (CEI) and cannot adapt to different discomfort thresholds properly.

5.2.4. Discomfort threshold tracking

We now consider the scenario where the discomfort threshold is time-varying, which can happen in practice. For example, when occupants change, new occupants may be willing to trade off more temperature deviations for more

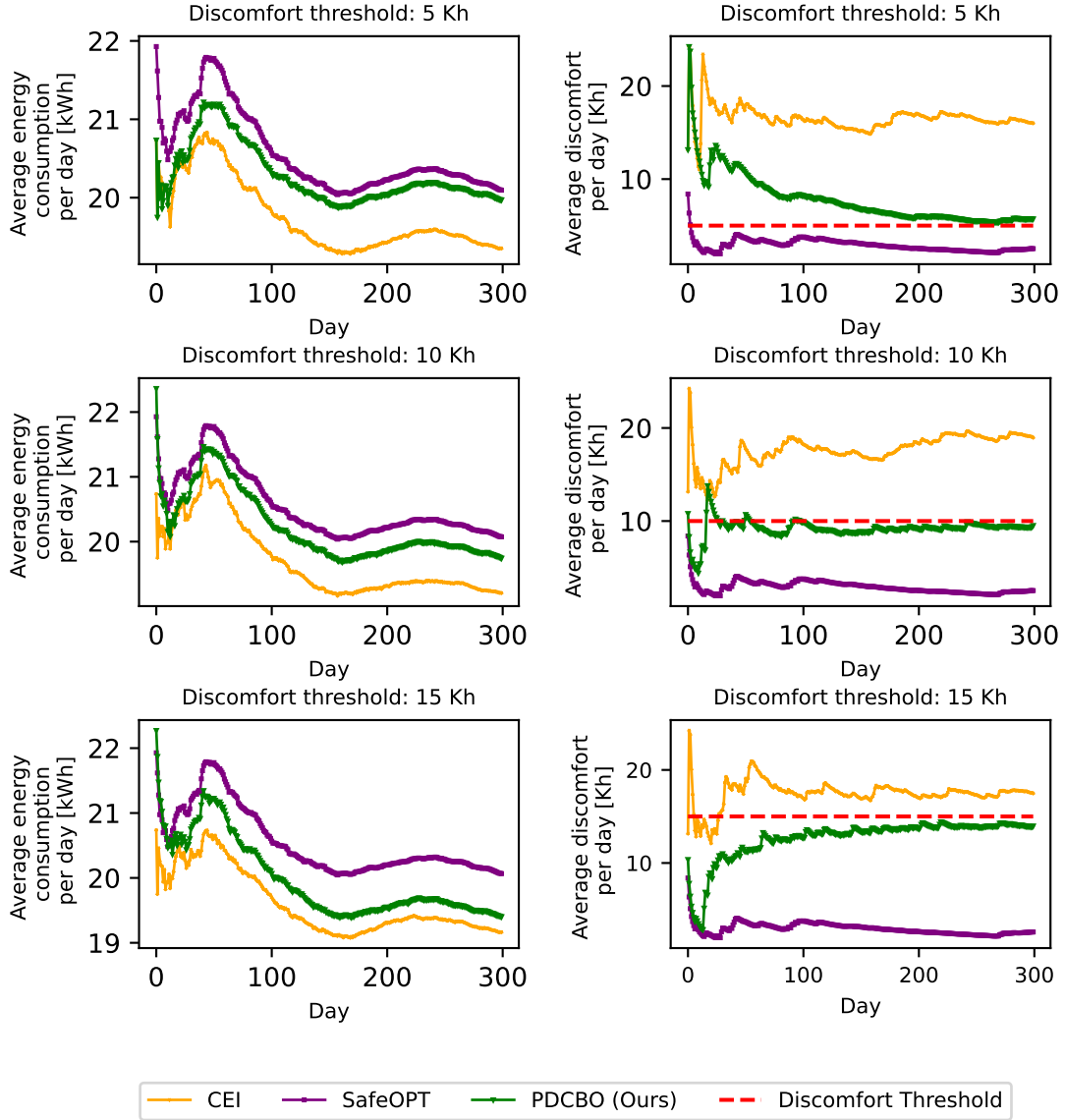


Figure 5: Average energy consumption E_n^{avg} and discomfort D_n^{avg} per day with discomfort threshold as 5K h, 10K h and 15K h per day. Note that the day-time energy consumption is doubled to reflect the real-world energy tariff.

energy savings, or vice versa. Fig. 8a shows the evolution of the average energy consumption and thermal discomfort with a time-varying discomfort threshold. The discomfort threshold is changed on days 75, 150, and 225. Every time the threshold changes, we reinitialize the calculation of the running average for the discomfort and energy consumption. However, we keep the algorithm continuously running, only modifying the constraint. For reference, Fig. 8b depicts the average ambient temperature during the four periods with different discomfort thresholds. We observe that periods 1 and 3, as well as periods 2 and 4, have similar ambient temperatures. Consequently, we focus our analysis on comparing periods 3 and 1 and between periods 4 and 2, respectively.

Interestingly, PDCBO closely tracks the change of discomfort threshold (Fig. 8a, right) and exploits the more and

more allowable temperature deviations to gradually reduce energy consumption, (comparing period 3 to 1 or period 4 to 2 in Fig. 8c). Note that the energy increase in period 3 (from about day 150 to day 225) as compared to period 2 is due to the decrease of ambient temperature (see Fig. 8b). In contrast and similarly to what was observed in the previous sections, the CEI method is overly aggressive and fails to respect the time-varying discomfort threshold most of the time. SafeOPT, on the contrary, is overly cautious and fails to exploit the time-varying discomfort threshold to reduce the energy consumption. When the discomfort threshold changes, we reset the running averages of energy consumption and discomfort, leading to some spikes in these two metrics.

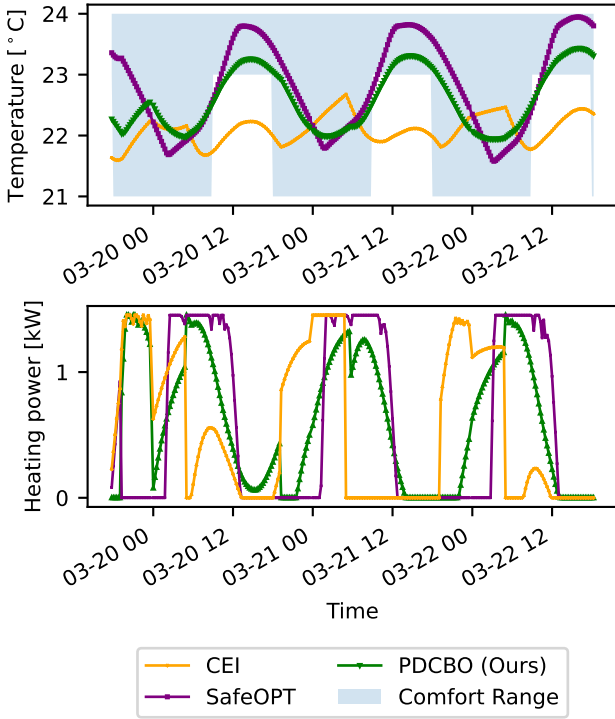


Figure 6: Three-day sample trajectories of the room temperature and heating power. Here, CEI chooses some parameters that simply stops heating during the daytime to save energy, which causes severe discomfort.

5.3. Energy constrained discomfort minimization

In this section, we consider the regime where energy consumption is limited to a low budget due to, for example, the energy crisis [48], and the pressure of achieving carbon-neutrality targets on time [49], and we want to maximize the comfort of the occupants with this limited budget. As compared to Problem (4), it is more relevant to bound the average energy consumption for energy constraint (which directly relates to the electricity bill) during a period.

Fig. 9 shows the evolution of E_n^{avg} and D_n^{avg} for the three analyzed methods. It can be observed that PDCBO manages to keep the average energy consumption below the predefined energy consumption threshold in the long term for all three different energy budget constraints. In sharp contrast, CEI fails to respect the energy budget constraint and can incur an average energy consumption that is more than twice the prescribed energy budget in the long term. On the other hand, the budgeted energy consumption is well exploited by PDCBO to efficiently reduce the discomfort by respectively 46%, 53%, and 63%, for the three different energy budgets compared to the overly cautious SafeOPT method that tries to keep strictly low energy consumption all the time.

To understand the impact of the energy budget, Fig. 10 shows sampled temperature trajectories (after running for about 200 days) of PDCBO with three different thresholds. It can be observed that as we gradually increase the budget,

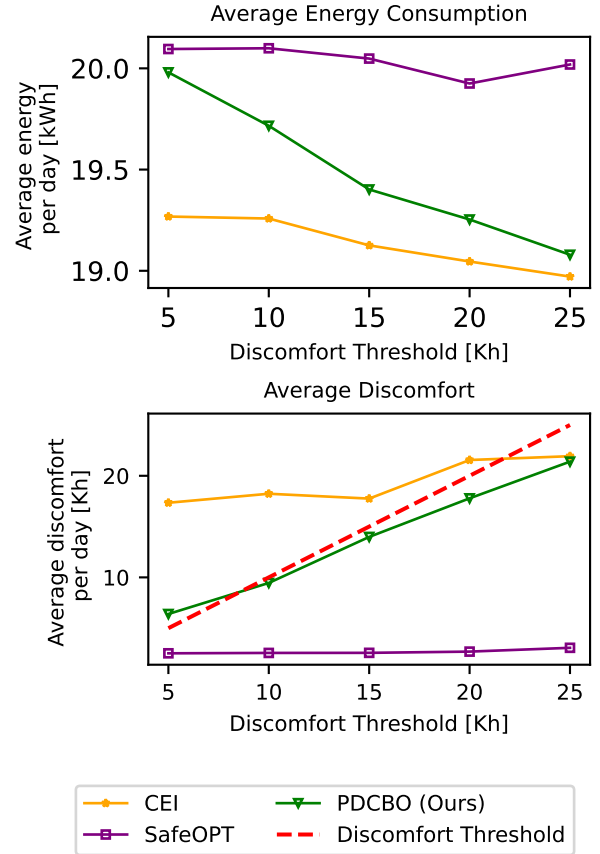


Figure 7: Sensitivity analysis to show the impact of different discomfort thresholds on the final average energy consumption (E_{300}^{avg} as defined in Eq. (6a)) and the final average discomfort per day (D_{300}^{avg} as defined in Eq. (6b)) over 300 days. Note that the daytime energy consumption is doubled here to reflect the real-world electricity price tariff.

the trajectories become better and better and incurs less and less discomfort.

6. Conclusion and discussion

In this paper, we presented a data-driven primal-dual contextual Bayesian optimization (PDCBO) approach to automatically tuning the parameters of a PI controller, the daytime setpoint of the temperature, and the pre-heating time to minimize the energy consumption of a room subject to a thermal discomfort constraint, or minimize the discomfort subject to an energy budget constraint. We showcased how PDCBO is able to simultaneously adapt to the time-varying ambient conditions and optimize the objective while satisfying constraints on average.

When minimizing the energy consumption subject to a thermal discomfort constraint, simulation results show that PDCBO can decrease the energy consumption by up to 4.7% compared to state-of-the-art safe Bayesian optimization methods while keeping the average discomfort below the given tolerable threshold. Additionally, it can automatically track time-varying tolerable thresholds. On

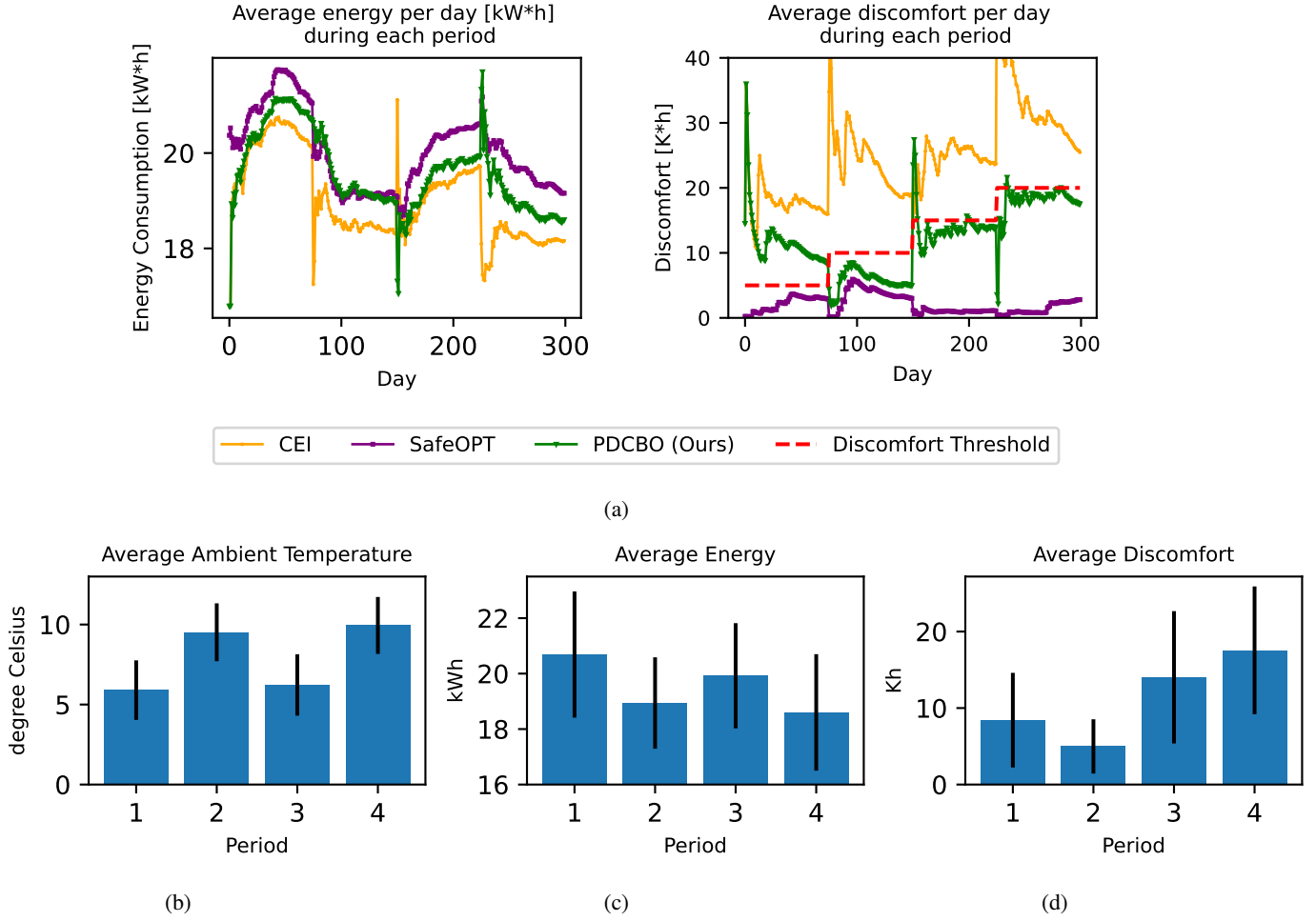


Figure 8: Discomfort tracking results. (a) Average energy and discomfort per day with time-varying discomfort threshold. The average on day t is taken from day $\tau_0(t)$ to t , where $\tau_0(t)$ is the day when the discomfort threshold on day t starts. (b)(c)(d) Average ambient temperature/energy consumption/discomfort during the four periods with different discomfort thresholds. Standard deviations are represented as the black lines.

the other hand, the other two constrained Bayesian optimization methods are either too cautious (SafeOPT) or overly aggressive (CEI) and cannot adapt to different discomfort thresholds properly.

When we instead optimize the thermal comfort of the occupants subject to a limited energy budget, PDCBO could reduce the average discomfort by up to 63% compared to SafeOPT, with an average energy consumption below the given budget. On the other hand, although it achieves lower discomfort, CEI severely violates the energy budget constraint.

One promising direction to further increase the sample efficiency of BO controller tuning could be to exploit the grey-box nature of the energy/discomfort functions (see Eq. (2) and Eq. (1), which are integrations of a black-box function) to accelerate the tuning of a building controller. Another direction is considering multi-zone building controller tuning, where the layout and geometrical information of the zones may be exploited to improve the

tuning efficiency using the recently proposed grey-box BO method [50].

Acknowledgements

This research was supported by the Swiss National Science Foundation under NCCR Automation, grant agreement 51NF40_180545, and in part by the Swiss Data Science Center, grant agreement C20-13.

Declaration of competing interests

The authors declare that they have no known competing financial interests or personal relationships that could have appeared to influence the work reported in this paper.

CRediT authorship contribution statement

Wenjie Xu: Conceptualization, Methodology, Software, Validation, Formal analysis, Data Curation, Visualization,

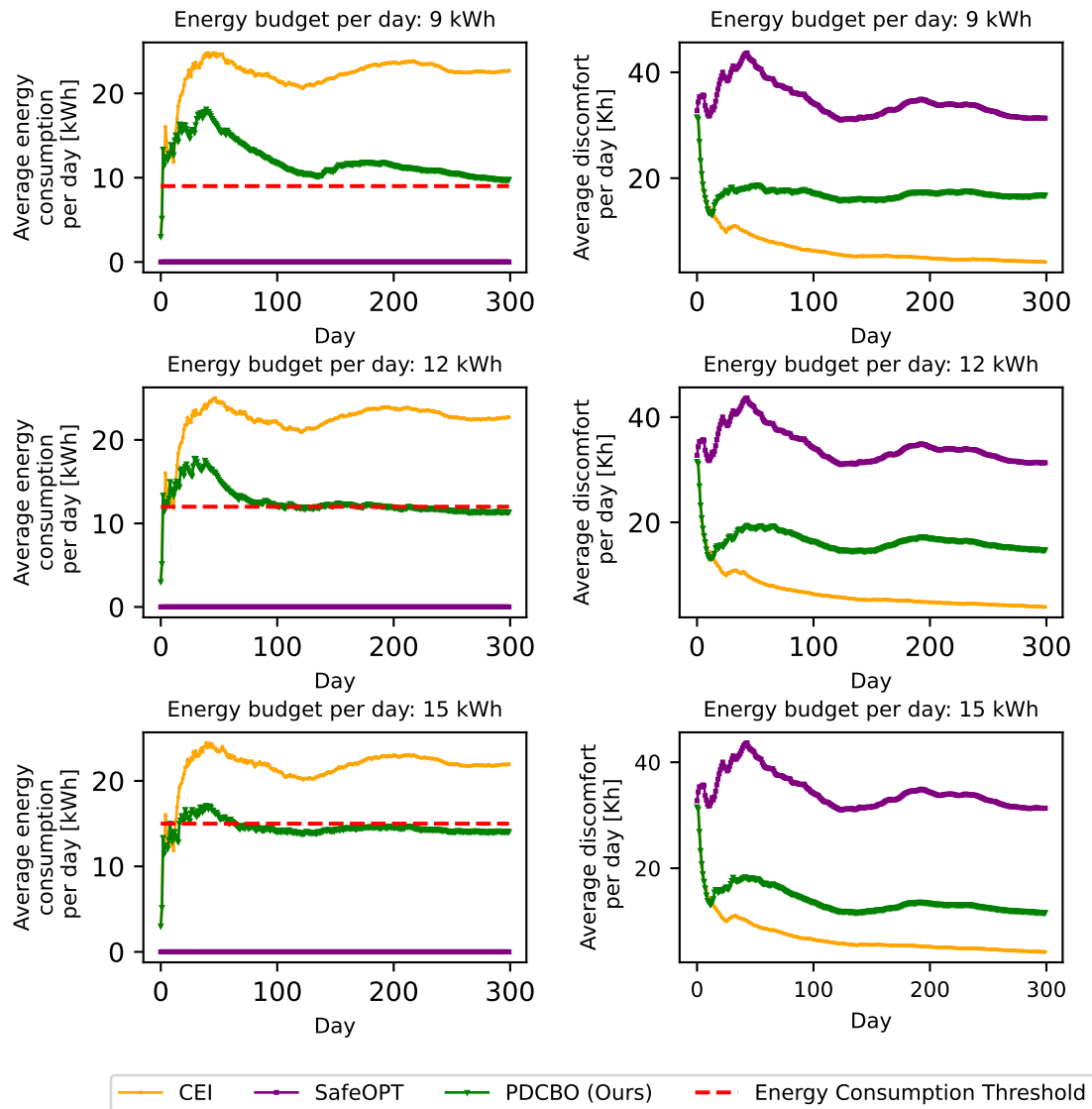


Figure 9: Average energy consumption and discomfort with limited average energy consumption budget as 9kWh, 12kWh and 15kWh per day shown in dashed red.

Writing - Original Draft. **Bratislav Svetozarevic:** Conceptualization, Methodology, Writing - Review & Editing, Supervision. **Loris Di Natale:** Software, Validation, Data Curation, Visualization, Writing - Review & Editing. **Philipp Heer:** Writing - Review & Editing, Resources, Funding acquisition. **Colin N Jones:** Conceptualization, Methodology, Writing - Review & Editing, Supervision.

References

- [1] A. Boodi, K. Beddiar, M. Benamour, Y. Amirat, M. Benbouzid, Intelligent systems for building energy and occupant comfort optimization: A state of the art review and recommendations, *Energies* 11 (2018) 2604.
- [2] F. Oldewurtel, A. Parisio, C. N. Jones, D. Gyalistras, M. Gwerder, V. Stauch, B. Lehmann, M. Morari, Use of model predictive control and weather forecasts for energy efficient building climate control, *Energy and Buildings* 45 (2012) 15–27.
- [3] T. Xiao, F. You, Building thermal modeling and model predictive control with physically consistent deep learning for decarbonization and energy optimization, *Applied Energy* 342 (2023) 121165.
- [4] Y. Gao, S. Miyata, Y. Akashi, Energy saving and indoor temperature control for an office building using tube-based robust model predictive control, *Applied Energy* 341 (2023) 121106.
- [5] B. Svetozarevic, C. Baumann, S. Muntwiler, L. Di Natale, M. N. Zeilinger, P. Heer, Data-driven control of room temperature and bidirectional EV charging using deep reinforcement learning: Simulations and experiments, *Applied Energy* 307 (2022) 118127.
- [6] Y. Lei, S. Zhan, E. Ono, Y. Peng, Z. Zhang, T. Hasama, A. Chong, A practical deep reinforcement learning framework for multivariate occupant-centric control in buildings, *Applied Energy* 324 (2022) 119742.
- [7] L. Yang, Z. Nagy, P. Goffin, A. Schlueter, Reinforcement learning for optimal control of low exergy buildings, *Applied Energy* 156 (2015) 577–586.
- [8] D. Coraci, S. Brandi, T. Hong, A. Capozzoli, Online transfer learning strategy for enhancing the scalability and deployment of deep reinforcement learning control in smart buildings, *Applied Energy* 333

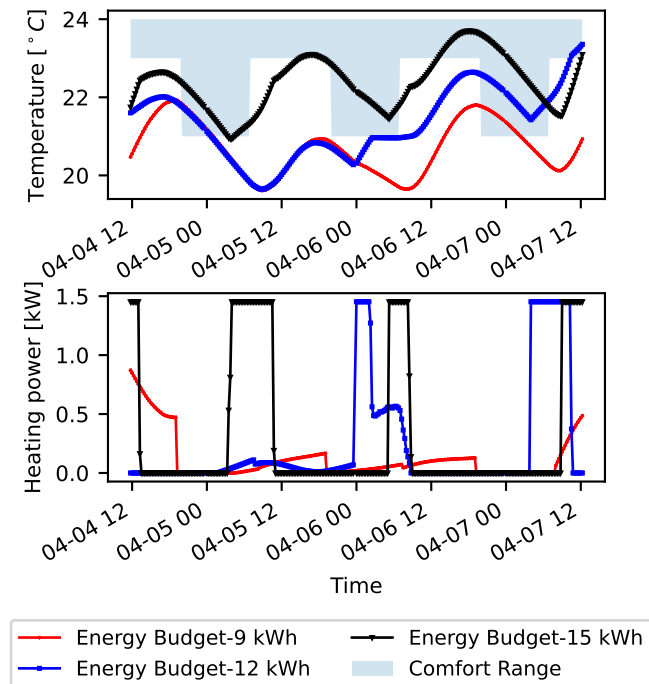


Figure 10: Sample trajectories of room temperature and the corresponding heating power with limited average energy consumption budget as 9kWh, 12kWh and 15kWh per day.

- (2023) 120598.
- [9] R. Shen, S. Zhong, X. Wen, Q. An, R. Zheng, Y. Li, J. Zhao, Multi-agent deep reinforcement learning optimization framework for building energy system with renewable energy, *Applied Energy* 312 (2022) 118724.
- [10] T. I. Salsbury, A survey of control technologies in the building automation industry, *IFAC Proceedings Volumes* 38 (2005) 90–100.
- [11] P. Stluka, G. Parthasarathy, S. Gabel, T. Samad, Architectures and algorithms for building automation—an industry view, in: *Intelligent Building Control Systems*, Springer, 2018, pp. 11–43.
- [12] M. Fiducioso, S. Curi, B. Schumacher, M. Gwerder, A. Krause, Safe contextual Bayesian optimization for sustainable room temperature PID control tuning, in: *Proceedings of the Twenty-Eighth International Joint Conference on Artificial Intelligence, International Joint Conferences on Artificial Intelligence*, pp. 5850–5856.
- [13] K. Yan, X. Zhou, B. Yang, AI and IoT applications of smart buildings and smart environment design, construction and maintenance, 2023.
- [14] W. Xu, C. N. Jones, B. Svetozarevic, C. R. Laughman, A. Chakrabarty, VABO: Violation-Aware Bayesian Optimization for closed-loop control performance optimization with unmodeled constraints, in: *2022 American Control Conference (ACC)*, IEEE, pp. 5288–5293.
- [15] W. Xu, C. N. Jones, B. Svetozarevic, C. R. Laughman, A. Chakrabarty, Violation-aware contextual Bayesian optimization for controller performance optimization with unmodeled constraints, *arXiv preprint arXiv:2301.12099* (2023).
- [16] D. R. Jones, M. Schonlau, W. J. Welch, Efficient global optimization of expensive black-box functions, *J. Global Optim.* 13 (1998) 455–492.
- [17] W. Xu, Y. Jiang, E. T. Maddalena, C. N. Jones, Lower bounds on the worst-case complexity of efficient global optimization, *arXiv preprint arXiv:2209.09655* (2022).
- [18] W. Xu, Y. Jiang, B. Svetozarevic, C. N. Jones, Primal-dual contextual Bayesian optimization for control system online optimization with time-average constraints, in: *2023 IEEE 62nd Conference on Decision and Control (CDC)*, IEEE.
- [19] B. Chen, Z. Cai, M. Bergés, Gnu-RL: A precocial reinforcement learning solution for building HVAC control using a differentiable MPC policy, in: *Proceedings of the 6th ACM International Conference on Systems for Energy-Efficient Buildings, Cities, and Transportation*, pp. 316–325.
- [20] Y. Shen, Y. Pan, BIM-supported automatic energy performance analysis for green building design using explainable machine learning and multi-objective optimization, *Applied Energy* 333 (2023) 120575.
- [21] H. Yan, G. Ji, K. Yan, Data-driven prediction and optimization of residential building performance in Singapore considering the impact of climate change, *Building and Environment* 226 (2022) 109735.
- [22] Q. Jin, M. Overend, Facade renovation for a public building based on a whole-life value approach, in: *Proceedings of Building Simulation and Optimisation Conference*, Loughborough, UK, p. 378e85.
- [23] C. Diakaki, E. Grigoroudis, N. Kabelis, D. Kolokotsa, K. Kalaitzakis, G. Stavrakakis, A multi-objective decision model for the improvement of energy efficiency in buildings, *Energy* 35 (2010) 5483–5496.
- [24] F. P. Chantrelle, H. Lahmidi, W. Keilholz, M. El Mankibi, P. Michel, Development of a multicriteria tool for optimizing the renovation of buildings, *Applied Energy* 88 (2011) 1386–1394.
- [25] A.-T. Nguyen, S. Reiter, P. Rigo, A review on simulation-based optimization methods applied to building performance analysis, *Applied Energy* 113 (2014) 1043–1058.
- [26] X. Li, J. Wen, Review of building energy modeling for control and operation, *Renewable and Sustainable Energy Reviews* 37 (2014) 517–537.
- [27] S. Zhan, G. Wichern, C. Laughman, A. Chong, A. Chakrabarty, Calibrating building simulation models using multi-source datasets and meta-learned Bayesian optimization, *Energy and Buildings* 270 (2022) 112278.
- [28] A. Chakrabarty, E. Maddalena, H. Qiao, C. Laughman, Scalable Bayesian optimization for model calibration: Case study on coupled building and HVAC dynamics, *Energy and Buildings* 253 (2021) 111460.
- [29] A. Bhattacharya, S. Vasisht, V. Adetola, S. Huang, H. Sharma, D. L. Vrabie, Control co-design of commercial building chiller plant using Bayesian optimization, *Energy and Buildings* 246 (2021) 111077.
- [30] W. Xu, Y. Jiang, B. Svetozarevic, C. Jones, CONFIG: Constrained efficient global optimization for closed-loop control system optimization with unmodeled constraints, *IFAC-PapersOnLine* (2023).
- [31] B. Jiang, M. D. Berliner, K. Lai, P. A. Asinger, H. Zhao, P. K. Herring, M. Z. Bazant, R. D. Braatz, Fast charging design for lithium-ion batteries via Bayesian optimization, *Applied Energy* 307 (2022) 118244.
- [32] M. Lisicki, W. Lubitz, G. W. Taylor, Optimal design and operation of archimedes screw turbines using Bayesian optimization, *Applied Energy* 183 (2016) 1404–1417.
- [33] M. A. Gelbart, J. Snoek, R. P. Adams, Bayesian optimization with unknown constraints, in: *Proc. of the 30th Conf. on Uncertainty in Artif. Intell., UAI'14*, AUAI Press, Arlington, Virginia, USA, 2014, p. 250–259.
- [34] J. R. Gardner, M. J. Kusner, Z. E. Xu, K. Q. Weinberger, J. P. Cunningham, Bayesian optimization with inequality constraints., in: *Proc. of the Int. Conf. on Mach. Learn.*, volume 2014, pp. 937–945.
- [35] Y. Sui, A. Gotovos, J. Burdick, A. Krause, Safe exploration for optimization with Gaussian processes, in: *Proc. of the Int. Conf. on Mach. Learn.*, pp. 997–1005.
- [36] X. Zhou, B. Ji, On kernelized multi-armed bandits with constraints, in: *Advances in Neural Information Processing Systems*.
- [37] M. Taleghani, M. Tenpierik, S. Kurvers, A. Van Den Dobbelsteen, A review into thermal comfort in buildings, *Renewable and Sustainable Energy Reviews* 26 (2013) 201–215.
- [38] C. E. Rasmussen, Gaussian processes in machine learning, in: *Summer school on machine learning*, Springer, pp. 63–71.
- [39] C. K. Williams, C. E. Rasmussen, Gaussian processes for machine learning, volume 2, MIT press Cambridge, MA, 2006.
- [40] P. I. Frazier, A tutorial on Bayesian optimization, *arXiv preprint arXiv:1807.02811* (2018).

- [41] N. Srinivas, A. Krause, S. M. Kakade, M. W. Seeger, Information-theoretic regret bounds for Gaussian process optimization in the bandit setting, *IEEE Transactions on Information Theory* 58 (2012) 3250–3265.
- [42] J. Nocedal, S. J. Wright, *Numerical optimization*, Springer, 1999.
- [43] L. Di Natale, B. Svetozarevic, P. Heer, C. N. Jones, Physically consistent neural networks for building thermal modeling: theory and analysis, *Applied Energy* 325 (2022) 119806.
- [44] L. Di Natale, B. Svetozarevic, P. Heer, C. N. Jones, Towards scalable physically consistent neural networks: An application to data-driven multi-zone thermal building models, *Applied Energy* 340 (2023) 121071.
- [45] EWZ, Current tariffs for the city of Zurich, <https://www.ewz.ch/en/private-customers/electricity/tariffs/overview-of-tariff.html>, since 2023.
- [46] GPpy, GPpy: A Gaussian process framework in python, <http://github.com/SheffieldML/GPy>, since 2012.
- [47] Z. Wang, R. de Dear, M. Luo, B. Lin, Y. He, A. Ghahramani, Y. Zhu, Individual difference in thermal comfort: A literature review, *Building and Environment* 138 (2018) 181–193.
- [48] <https://www.energypriceindex.com/price-data>, 2022.
- [49] <https://www.un.org/en/climatechange/net-zero-coalition>, 2022.
- [50] W. Xu, Y. Jiang, B. Svetozarevic, C. N. Jones, Bayesian optimization of expensive nested grey-box functions, *arXiv preprint arXiv:2306.05150* (2023).